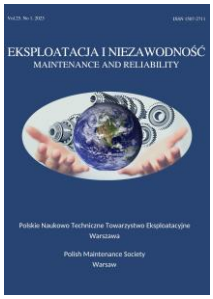

Eksploatacja i Niezawodnosc – Maintenance and Reliability

Volume 25 (2023), Issue 1

journal homepage: http://www.ein.org.pl

Article citation info:
Radek N, Michalski M, Mazurczuk R, Szczodrowska B, Plebankiewicz I, Szczepaniak M. Operational tests of coating systems in military technology applications. Eksploatacja i Niezawodnosc – Maintenance and Reliability 2023: 25(1) http://doi.org/10.17531/ein.2023.1.12

Indexed by:

Operational tests of coating systems in military technology applications

Norbert Radek[a*], Marek Michalski[b], Robert Mazurczuk[c], Bogusława Szczodrowska[c], Ireneusz Plebankiewicz[c], Marcin Szczepaniak[c]

[a] Wydział Mechatroniki i Budowy Maszyn Politechnika Świętokrzyska 25-314 Kielce Poland
[b] F.H. Barwa 25-253 Kielce Poland
[c] Wojskowy Instytut Techniki Inżynieryjnej 50-961 Wrocław Poland

Highlights

- military green paint was modified with carbon nanotubes and spherical iron,
- an original technology for the production of multi-layer coating systems was developed,
- satisfactory attenuation coefficients for radar waves were noted for the radar-absorbing coating systems,
- good adhesion of the coating systems and their low roughness were demonstrated,
- an original multi-criteria method of testing the operational properties of paint systems was used.
- paint systems can potentially be used on armaments and military equipment.

Abstract

The paper presents an analysis of the functional operational properties of multilayer coatings for use in military technology in the field of masking. The developed coating systems are characterized by operational innovation due to their small thickness when compared to those currently used by global defence contractors while maintaining the re-emission coefficient required for camouflage to be effective in the optical range. Their service life and durability were assessed in terms of functional properties based on measurements of attenuation coefficients, surface geometric structure, adhesion, specular gloss and colour parameters. The tests were carried out for coating systems fabricated in five variants: a two-layer paint system (SP1), a three-layer paint system (SP2), a laser-modified three-layer paint system (SP3) and a four-layer paint system in two variants (SP4 and SP5), with the former being modified with carbon nanotubes and the later – with spherical iron. Coating systems are characterized by low roughness and good adhesion and have appropriate attenuation coefficients for radar waves. Due to their operational properties, the developed coating systems can be used on armaments and military equipment.

Keywords
coating system, functional properties, armaments and military equipment

1. Introduction

The dynamic development of technology related to the operation of electronic products and information technology results in imposing new, higher operational and technical requirements on radars. In the 1950s, the Polish Armed Forces were equipped with NYSA-A radars operating in the 600 MHz band and on a 50 cm wavelength, and NYSA-B radar (Radiolocation Altitude Measurement Station) with a range of 150 km and equipped with parabolic antennas.

Currently, works are underway to equip the Polish Army with modern TRS-15 surveillance radars for detecting and tracking targets, and RZRA LIWIEC counter-battery radars intended for detecting and identifying active enemy artillery fire stations. Modern TRS-15 radars are three-coordinate radars, capable of determining the range, altitude and azimuth and operating in the S-band frequency range (2÷4 GHz). They allow simultaneous tracking of 255 targets at a maximum distance of 240 km and an altitude of up to 30 km. A vital component of contemporary radars is the "friend or foe" identification system.

A natural defensive reflex is to create an effective system to delay the detection of objects in the area of operation thus reducing the probability of detection. This process can be implemented already at the technical design stage, but this applies to newly developed devices only. In the case of equipment which already is in service with the Polish Armed

(*) Corresponding author.
E-mail addresses: N. Radek (ORCID: 0000-0002-1587-1074) norrad@tu.kielce.pl, M. Michalski (ORCID: 0000-0003-0419-7886), mmichalski@barwa.kielce.pl, R. Mazurczuk (ORCID: 0000-0001-7791-9929) mazurczuk.r@witi.wroc.pl, B. Szczodrowska (ORCID: 0000-0001-5480-8046) szczodrowska@witi.wroc.pl, I. Plebankiewicz (ORCID: 0000-0002-0077-5215) plebankiewicz@witi.wroc.pl, M. Szczepaniak (ORCID: 0000-0003-4313-3703) szczepaniak@witi.wroc.pl

Forces, the coating systems containing materials with a high microwave radiation absorption coefficient should be used, ones with a structure guaranteeing a high scattering coefficient. Awareness of the above-mentioned coefficients is the basis for developing appropriate camouflage solutions in this area.

The basic factor determining the detectability of the object in the radar range is the possibility of recording the signal generated by the transmitter after it has been reflected from objects in the field of view. The reflection intensity depends mainly on the material with which the object was manufactured and its shape and orientation in space in relation to the radar station. These factors determine the so-called radar cross-section (also known as radar signature) of the object (expressed in units of surface area), the value of which affects the possibility of distinguishing the object from its background by a given radar station.

It can be generally stated that an object with a larger radar cross-section is more easily distinguished from its background (with other detectability conditions remaining unchanged). The detection range depends on the following factors:

- transmitter power;
- antenna directive gain;
- the effective surface of the receiving antenna;
- the object radar cross-section.

The first three factors characterize the surveillance device. The users of the equipment that is under surveillance have no direct impact on them. In this situation, the only means of counteracting is to reduce the radar cross-section of the object, limiting its detection range.

Assuming that the detection of objects depends on their ability to reflect waves, the general range equation assumes the following form [6]:

$$R_{max} = \sqrt[4]{\frac{Pn \times G \times \delta \times A}{(4\times\pi)^2 \times Po_{min}}} \quad (1)$$

where:

R_{max} – maximum detection range [m],
A – effective aperture (area) of the receiving antenna [m^2],
G – antenna gain [-],
Pt – power transmitted by the radar [W],
δ – target radar cross-section [m^2],
Po_{min} – min. power received at which the object can still be distinguished from the noise (threshold power – one of the properties of the receiver) [W].

Decrease of the radar cross-section of the given object can be done via [9, 19]:

- the change of the spatial arrangement of the object;
- the use of highly lossy materials (with low reflectivity) for the housings/casings;
- use of barriers made of highly lossy materials (not directly connected with the object) to conceal the object,
- the use of additional layers (cladding) made with materials characterised by high loss (low reflectivity) on the external surface of the objects.

Most of these recommendations were used as part of the "stealth" technology used in the production of the American so-called stealth bombers and fighters [3]. Their radar cross section has been reduced by about a hundred times (from 100 m^2 to about 1m^2). Indeed, aircrafts made with stealth technology are not completely invisible to the radar, but their detection range has been reduced several times. Figure 1 shows the American Lockheed *F-117 Nighthawk* stealth attack aircraft (in the "bomber" version), while Figure 2 shows the Lockheed *SR-71 Blackbird* strategic reconnaissance and patrol aircraft. The *F-117 Nighthawk* and *SR-71 Blackbird* aircrafts have appropriate angled surfaces of the flat sheets, which results in partial scattering of radio waves and are more difficult to detect by radars.

Fig. 1. Lockheed F-117 Nighthawk bomber [2]

Fig. 2. Lockheed SR-71 Blackbird strategic reconnaissance and patrol aircraft [14]

Stealth technology is widely used in the design of modern devices for which a reduction of the detection distance is required. In the case of products that have already been put into operation, obtaining the scattering of the reflected beam (reducing the radar cross-section of the object) via modification of the shape of the surface is most often impossible, and in such cases, external coatings can be used in the form of, for example, paint systems or shields attached to the object.

Currently, there is a dynamic development of coating production processes using various surface engineering technologies, such as: plasma spraying [37], HVOF spraying [38], ESD method [33], laser cladding [41], laser alloying [32], physical vapor deposition [12], chemical vapor deposition [8], which mainly perform protective and anti-wear functions.

The evolution of paint coatings is quite rapid, multidirectional and most interesting [11]. The progress in the field of polymer coating technology stems from the three most important functions, i.e. the decorative function [34], the protective function [10, 21] and the informative function [17]. Paint systems account for approximately 50% of all coating systems. It is estimated that about 95% of steel structures are

safeguarded against corrosion with protective coatings, including as much as 90% – with paint coatings [4]. The service life of paint systems ranges from several months to several years [13].

A special group of paint systems are paint coatings for military applications, mainly for camouflaging weapon systems and military equipment [39]. Paint coatings are fundamentals of camouflage – they camouflage vehicles/objects in the optical range, both in visible light (VIS) and in the near-infrared (NIR) range [31]. The main task of effective camouflage is to eliminate those features, which may cause the object to be differentiated from its surroundings [30], i.e. those that make it possible to distinguish one's own assets from the background, and these may include, for example, colour, shape, size, gloss and texture [35, 40].

As part of the cooperation between the F.H. BARWA company, Kielce University of Technology and the Military Institute of Engineer Technology (WITI) in Poland the companies have attempted to modify the green paint commonly used for camouflage paintings applied on the surface of objects. The aim behind their activities was to develop a coating system that would meet the camouflage requirements both in terms of spectral characteristics in the range from 350 nm to 1200 nm, colour coordinates, and camouflage objects in the radar range.

When selecting the composition of the paint and the method of its application, in order to create a coating system effective in camouflaging objects and protecting them against radar reconnaissance, the following were taken into account:

- reflection coefficient – reflection of the wave at the boundary of the media (mismatch of the wave impedance of the media), reflections at the boundaries between the media should also be taken into account;
- absorption coefficient – absorption of wave energy by the material;
- transmission coefficient – penetration of the wave through the material.

The analysis of the state of the art revealed that there are no scientific papers, neither published in Poland nor in international journals, on operational testing of radar-absorbing paint systems for military applications.

The paper presents the results of functional tests of paint systems developed with the use of carbon nanotubes and innovative spherical iron particles of appropriately selected shape and size and applied in a properly tailored multi-layer coating system. It is due to this solution that camouflage minimizing the detection of objects via radar reconnaissance is made possible using a system with a much smaller thickness compared to the currently used ones, and which can be employed in products for the military. As part of the ongoing research, reference was made to the measurements of attenuation coefficients, geometric structure of the surface, adhesion, specular gloss and colour parameters.

2. Experimental procedure

Samples for the application of coatings were made of S355 structural steel with dimensions of 300 mm x 300 mm x 1 mm. The surfaces of the steel samples were polished using a rotary machine with P80 sandpaper and washed with a solvent.

To prepare the surface and apply the paint systems, Festool's rotary polisher with abrasive paper from the same company, SATA GmbH & Co. KG spray guns with nozzles, and a Blowtherm spray booth were used. The cabin had the function of extracting the excess sprayed paint and was covered with foil and secured with a gel preventing dust from settling on the surface of the applied coating. In addition, it was equipped with a thermostat maintaining a constant temperature, with the possibility of increasing it to a temperature of about 60°C, which is required for drying large samples. For drying smaller samples, a WKL 64/70 temperature and climate test chamber with adjustable temperature and humidity by Weiss Umwlttechnik GmbH was used.

Five variants of radar-absorbent coating systems were applied onto the prepared steel samples via pneumatic spraying. These include:

1. a two-layer coating system (SP1): anti-corrosion primer, camouflage paint layer (green);
2. a three-layer coating system (SP2): anti-corrosion primer + carbon nanotubes (0.5 wt%), interlayer coating + carbon nanotubes (2 wt%), camouflage paint layer (green) + carbon nanotubes (0.5 wt%);
3. a three-layer coating system (SP3): anti-corrosion primer + carbon nanotubes (0.5 wt%), interlayer coating + carbon nanotubes (2 wt%), camouflage paint layer (green) + carbon nanotubes (0.5 wt%)). The coating system was laser-modified;
4. a four-layer coating system (SP4): anti-corrosion primer, interlayer coating + spherical iron (min. content), anti-corrosion primer, camouflage paint layer (green);
5. a four-layer coating system (SP5): anti-corrosion primer, interlayer coating + spherical iron (max. content), anti-corrosion primer, camouflage paint layer (green).

In the technological process, the following parameters for applying the camouflage topcoat (green paint) were used:

- surface temperature: 24÷26°C;
- working pressure 0.2÷0.25 MPa;
- evaporation time in between layer application: 15 minutes;
- dry film thickness: 60÷70 µm;
- application technique: pneumatic spraying;
- no. of applications: two layers;
- drying temperature: 60 °C;
- drying time: 60 minutes.

The remaining layers were applied following the technical data sheets provided by the manufacturer of a given paint.

Measurements of the thickness of paint systems were conducted using the magnetic induction method. Twelve measurements were made for each coating system, and that allowed the thickness results to be averaged. The average thicknesses of the applied systems was in the range of 1129÷2785 µm. The smallest thickness was found for the SP1 paint system (averaged thickness was g_{avr}=1129 µm), while the SP5 coating system was the thickest - g_{avr}=2785 µm. What is more, the highest thicknesses were found for the SP4 (g_{avr}=2549 µm) and SP5 paint systems, both of which contained spherical iron.

3. Experimental test results

3.1. Measurement of attenuation coefficient

The test stand with the SD-203TMS reflectometer was used to measure the attenuation of microwave radiation (Fig. 3). The SD-203TMS reflectometer is offered by the Geozondas company as a portable measurement system [1, 16]. However, the number of connections between individual devices, and most importantly, the need to precisely position the antennas in relation to each other and the measured sample, so far limits the scope of its application to laboratory measurements [42].

The walls of the laboratory room (Fig. 3a) were covered with a damping cover [7], ensuring a minimum microwave attenuation at the level of 12 dB. The positioning of the antennas and the reference plate in relation to the walls, the ground and the ceiling provides space for the propagation of radio waves (the principle of the Fresnel zone was maintained) [20, 36].

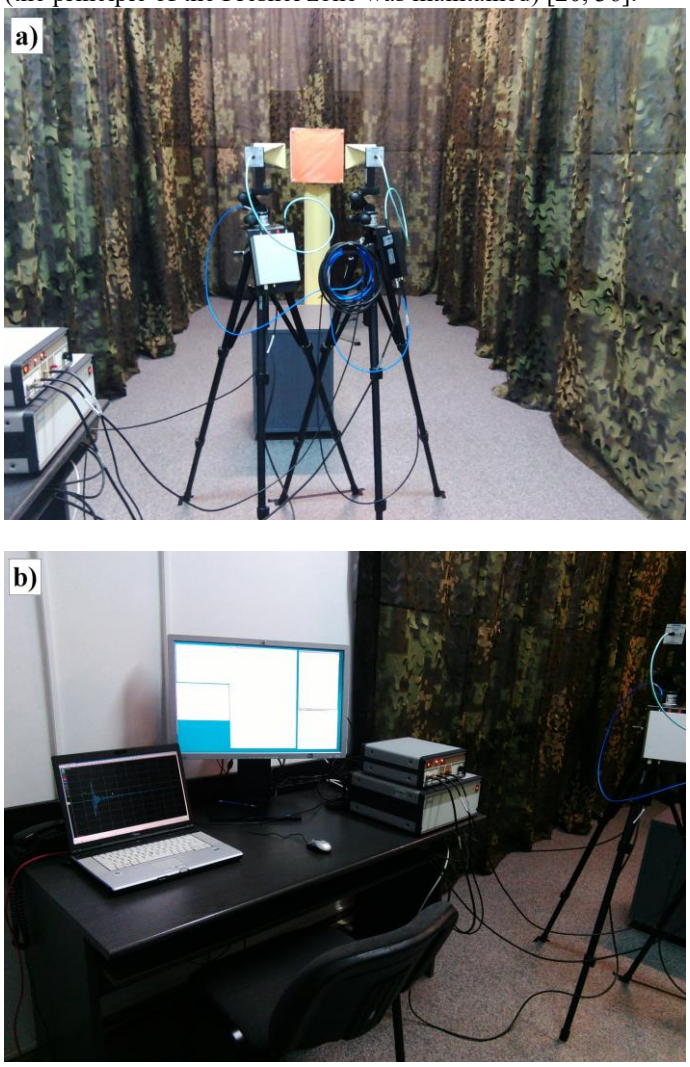

Fig. 3. Test stand at WITI for measuring the attenuation of microwave radiation with the SD-203TM reflectometer: a) antenna set, b) signal recording and processing station

The system enables the measurement of the reflection coefficient or attenuation of the absorbers in the frequency range from 4 to 18 GHz. The system operating principle is based on a picosecond pulse transmitted by the transmitting antenna, received by the receiving antenna as a signal reflected by the object and converted by the sampling head of the oscilloscope [2, 15].

In order to assess the effectiveness of the course of action taken, we examined whether the currently used paint system applied with the recommended thicknesses of the primer layer and the topcoat layer (SP1) maintained, provides any attenuation. The result of the attenuation measurement is presented in Figure 4. You can see that the level of attenuation of radar waves in the frequency range of 4÷18 GHz [5] was between -0.09 dB for 8.5 GHz and - 0.41 dB for 13.0 GHz.

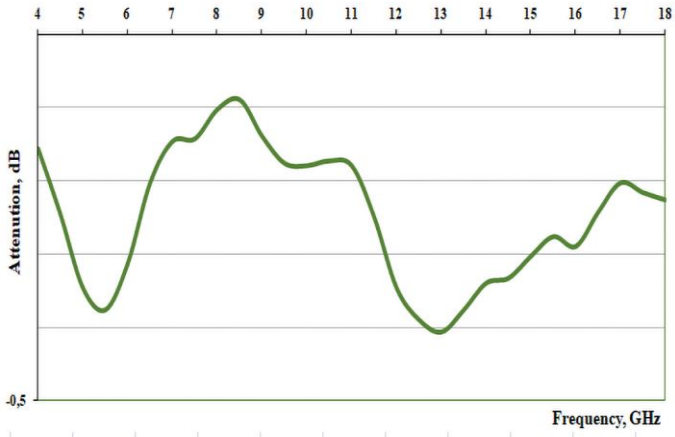

Fig. 4. Attenuation value for the SP1 coating system

In the course of further analyses on the increase in the attenuation of radar waves by the paint systems, we recognised that it was reasonable to perform tests with the use of additives in the form of absorbers added to the liquid product. In the first stage, the focus was on carbon nanotube-doped topcoat (SP2). The measurement result is shown in Figure 5.

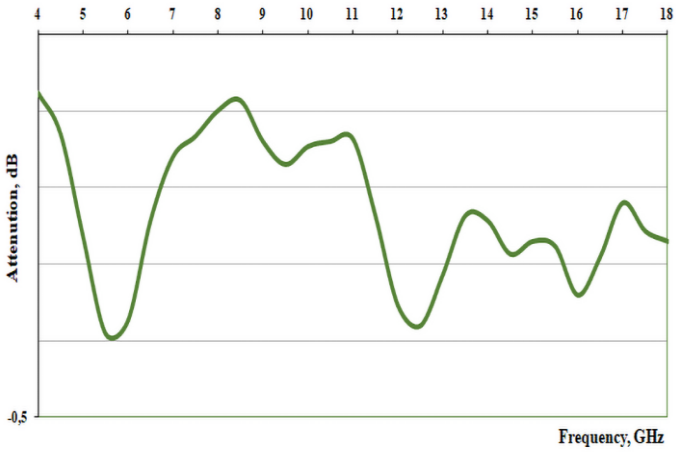

Fig. 5. Attenuation value for the SP2 coating system

For the coating with carbon nanotubes, the radar radiation attenuation was also insufficient and only a slight improvement in attenuation in the 16 GHz range was obtained.

Then, an attempt was made to check whether the modification of the topcoat (SP3) using a laser beam would increase the attenuation. Laser processing was performed with a model *ECL SS 200M* fibre laser, with the following parameters: laser output power? P = 100 W, feed rate v = 1 m/min, pulse repetition rate f = 20 kHz, rectangular beam size 1 mm x 100 mm, wavelength λ= 1064 nm, pulse mode. The measurement results are shown in Figure 6.

The attenuation curve (Fig. 6) changed somewhat, maintaining the same tendency as the attenuation curve in Figure 4. Laser modification of the paint coating did not result in a noteworthy improvement of the attenuation value.

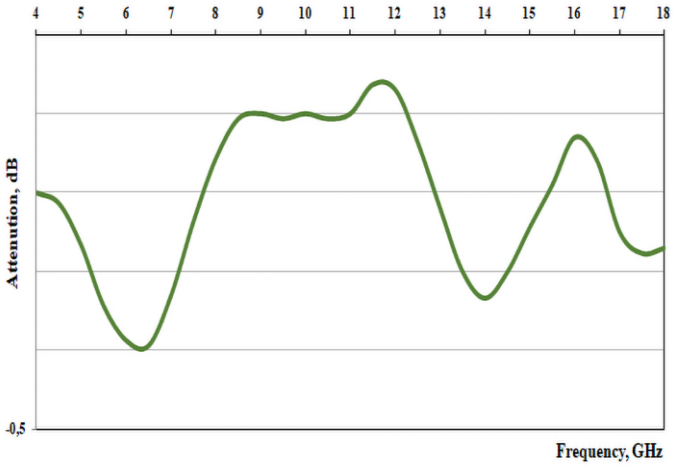

Fig. 6. Attenuation value for the SP3 coating system

The next stage involved tests using an absorber in the form of iron with a spherical molecular structure. The absorber was added to the intermediate coat under the topcoat. The SP4 coating system was prepared in accordance with the manufacturer's recommendations concerning the coating thickness and drying time. The results of the radar radiation suppression by the coating system consisting of, among others, an interlayer coating containing an absorber and a topcoat are shown in Figure 7.

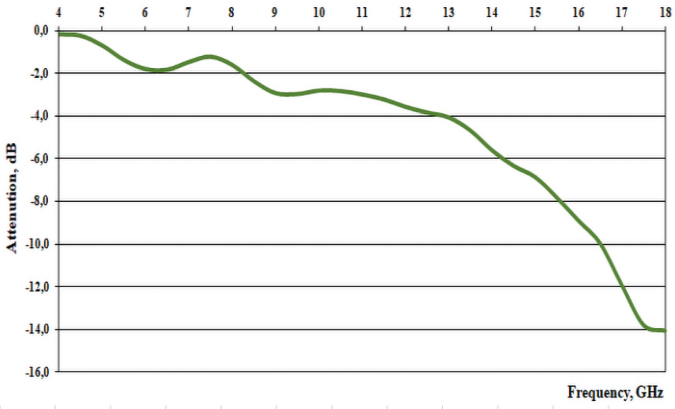

Fig. 7. Attenuation value for the SP4 coating system

Bearing in mind the results obtained so far and after extensive analysis, a decision was made to fabricate a sample with a coating of increased thickness and variable composition of individual layers (the content of spherical iron was increased). Following this theory, a SP5 coating system of larger thickness was manufactured. Figure 8 illustrates the results of the radio wave attenuation measurements for this particular coating system configuration.

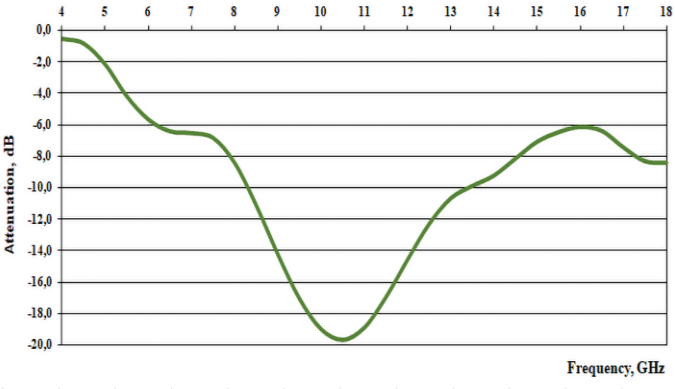

Fig. 8. Attenuation value for the SP5 coating system

The findings on the radar signal attenuation graph of paint coatings containing spherical iron are very promising (Fig. 7 and 8). The attenuation values obtained for frequencies above 6 GHz are within the range required for camouflage covers known as the Mobile Camouflage Kit (Polish acronym ZKM). In the course of further work, attempts should be made to increase the attenuation efficiency for bandwidths in the range below 6 GHz by e.g. optimizing the concentration of spherical ferrous material in the liquid product, monitoring the effect of the topcoat thickness and the number of layers (using wave reflection at the boundary of the media) on the attenuation of radar-absorbing coating systems.

3.2. Measurements of the surface geometric structure

Measurements of surface geometric structure (SGS) and roughness were carried out at the Laboratory of Computer Measurements of Geometric Quantities of the Kielce University of Technology. Measurements of surface stereometry were made using the Talysurf CCI optical profiler using the method of coherent correlation interferometry, enabling measurement with a z-axis resolution of up to 10 pm. The measurement result is saved in a matrix of 1024 x 1024 measurement points, which, with the lens used with a magnification of x50, gives the measured area of 0.33 mm x 0.33 mm and a horizontal resolution of 0.33 µm x 0.33 µm. Measurements were made using the function of numerical combination of nine measurements into a single surface (stitching). 10 measurements were made on each sample with radar-absorbing coating systems and S355 steel, which allowed to average the test results. The analysis of the obtained surface stereometry using the TalyMap Platinium software allowed for the assessment of the geometric structure of the tested surfaces.

Figures 9a÷9e show exemplary isometric images of the S-L surface geometrical structure (roughness) of the SP1, SP2, SP3, SP4, SP5 radar-absorbing coating systems obtained after applying the Gaussian filter 0.08 mm x 0.08 mm.

a)

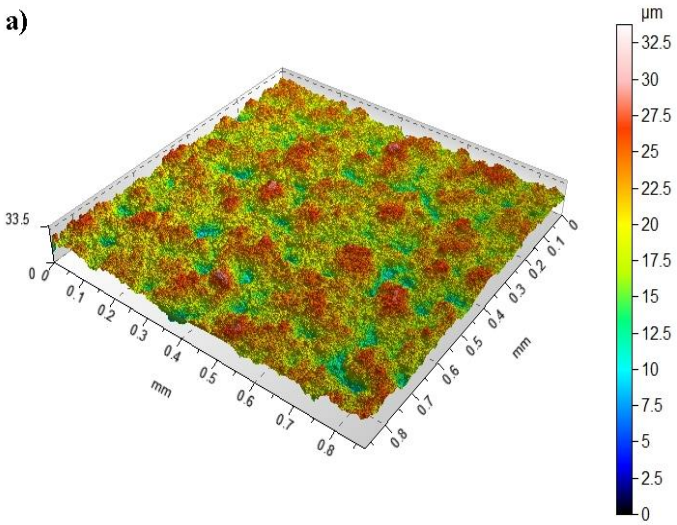

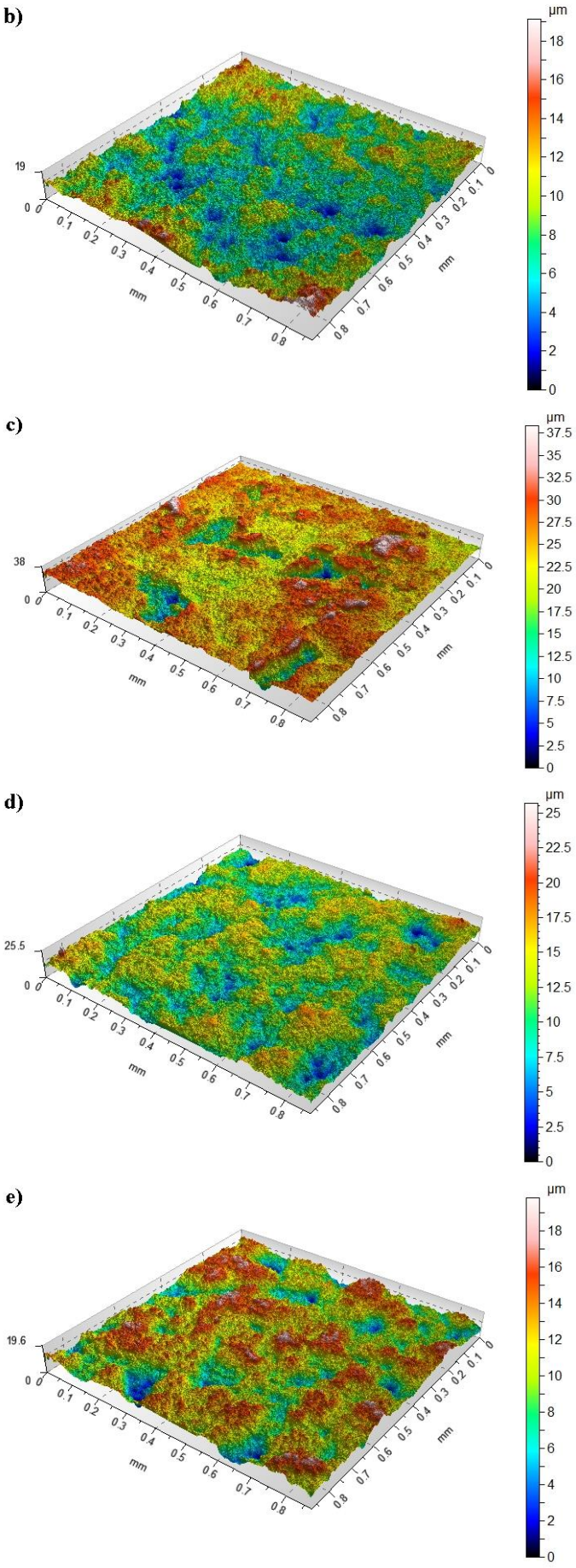

Fig. 9. Isometric images of S-L surfaces (roughness) of paint coating systems: a) SP1, b) SP2, c) SP3, d) SP4, e) SP5

Table 1 summarizes the most important averaged values of SGS parameters for the S-L surface.

Table 1. Averaged values of parameters of surface geometric structure S-L (roughness)

SGS parameters	Coating system				
	SP1	SP2	SP3	SP4	SP5
Sq, µm	3.208	2.448	4.605	2.782	2.928
Ssk	-0.358	0.500	-1.148	-0.304	-0.356
Sku	3.059	3.614	5.439	2.973	2.949
Sp, µm	13.644	11.211	13.951	14.158	8.556
Sv, µm	20.126	7.909	24.360	11.531	11.244
Sz, µm	33.770	19.120	38.311	25.688	19.800
Sa, µm	2.563	1.932	3.328	2.239	2.349

The tested radar-absorbing coating systems had averaged values of the arithmetic mean deviation of the surface roughness from the average surface *Sa*=1.932÷3.328 µm. The samples of S355 steel after grinding with P80 grain sandpaper, on which the coatings were applied, had *Sa*=1.131÷1.367 µm. The Sa parameter is the basic amplitude parameter for quantitative assessment of the condition of the analyzed surface. A similar tendency in the measurement results of radar-absorbing coating systems and S355 steel was observed for the mean square deviation of the surface roughness *Sq*, which was characterized by a strong correlation with the *Sa* parameter. As a result of the application of the masking topcoat, the surface roughness significantly increased.

Supplementary information on the shape of the surface of the tested elements is provided by the amplitude parameters: the coefficient of skewness - asymmetry *Sku* and the coefficient of concentration - kurtosis *Ssk*. These parameters are sensitive to the presence of local elevations or depressions on the surface, as well as defects (e.g. scratches, delaminations).

The obtained kurtosis values close to *Sku* = 3 prove that the distribution of ordinates for all samples is close to the normal distribution. The analysis of Table 1 shows that only the SP2 paint system has a positive value of the surface asymmetry coefficient *Ssk* (skewness), which proves that we are dealing with a smooth surface without deep scratches. Other masking coating systems have negative values of the skewness coefficient. The smallest value of the *Ssk* parameter measured for the SP3 radar-absorbing coating system results from the fact that there are numerous elevations and depressions on its surface, which is the result of the laser treatment.

3.3. Pull-off test adhesion measurements

In order to determine the adhesion strength with which the individual layers forming the coating system adhere to each other, adhesion measurements were carried out. The performed tests made it possible to determine the force with which the coating system should be acted on to lead to its tearing. An analysis of the nature of the rupture after the adhesion tests was also carried out. Adhesion measurements were made using an industry-standard pull-off test.

Pull-off test adhesion measurements according to EN ISO 4624:2016 [24] were performed in the laboratory of F. H. Barwa. The tests were carried out using the PosiTest AT hand-held adhesion meter by DeFelsko. The measurements consisted in gluing a standardized stamp to the surface of the coating system

using epoxy glue. Appropriate arrangement of punches on the surface of the system was maintained so that they were not too close to each other and to the edge of the sample. After 48 hours, complete cross-linking of the adhesive with the topcoat is considered. Then, after cleaning the coating surrounding the punch, the punch was broken using a measuring device and the value of the force was read. Two-component epoxy adhesive Araldite was used in the tests. Full cross-linking time acc. manufacturer is 48 hours at 23 °C. Aluminum punches with a diameter of ϕ20 mm were used. Radar-absorbing coating systems were applied to S355 steel samples with dimensions of 150 mm x 100 mm x 1 mm. 5 measurement tests were made for each coating system, which allowed for the averaging of test results. The obtained adhesion results along with the standard deviation are summarized in Table 2.

Table 2. Results of pull-off test adhesion measurements

Coating system	Adhesion, MPa	Adhesion average value, MPa	Standard deviation, MPa	Breakup type
SP1	2.16	2.31	040	Cohesive in the primer layer
	2.68			
	2.57			
	1.69			
	2.46			
SP2	2.44	2.68	0.20	Cohesive in the primer layer
	2.50			
	2.79			
	2.92			
	2.74			
SP3	3.04	2.41	0.44	Cohesive in the primer layer
	1.81			
	2.33			
	2.52			
	2.35			
SP4	1.87	2.35	0.60	Cohesive in the primer layer
	2.24			
	1.95			
	2.34			
	3.37			
SP5	3.13	3.42	0.60	Cohesive in the primer layer
	3.14			
	3.80			
	4.27			
	2.78			

The adhesion results of the coating systems were similar. The obtained test results show that the highest average value of adhesion (3.42 MPa) was characteristic of the SP5 paint system. The SP1 paint system with the lowest average value of adhesion (2.31 MPa) had approx. 33% less adhesion compared to the SP5 radar-absorbing coating system. The results of the adhesion measurements were characterized by low values of the standard deviation, which proves the high repeatability of the measurements. Figure 10 shows an exemplary view of the sample after the pull-off test adhesion measurements.

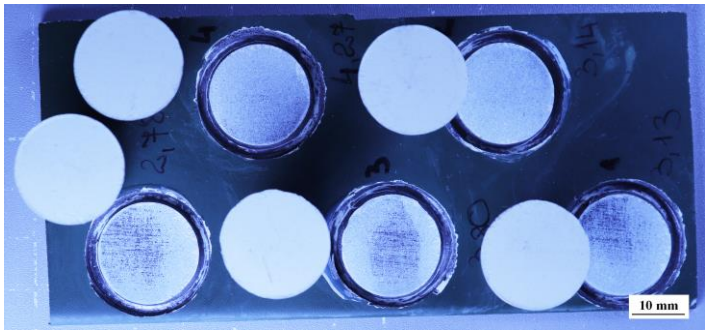

Fig. 10. View of the sample after measuring the adhesion of the SP5 paint coating system

3.3.1. Statistical analysis of adhesion measurement results

The adhesion test of the coating system was designed as a one-factor test, whereby, as in the case of the thickness test, the radar-absorbing coating system (SPP) was a factor controlled at 5 levels (painting systems SP1, SP2, SP3, SP4, SP5), and the adhesion was measured by pull-off test was the observed quantity (ADHESION designation). In order to reduce the impact of random uncontrolled factors, 5 replications were assumed (Table 3).

Table 3. Experimental design

Controlled size		Observed size
SPP		ADHESION
Horizontal	SP1	5 replications
	SP2	5 replications
	SP3	5 replications
	SP4	5 replications
	SP5	5 replications

After the tests, a total of 25 results were obtained (Table 4).

Table 4. Results of pull-off test adhesion measurements

SPP		SP1	SP2	SP3	SP4	SP5
Replication	1	2.16	2.44	3.04	1.87	3.13
	2	2.68	2.50	1.81	2.24	3.14
	3	2.57	2.79	2.33	1.95	3.80
	4	1.69	2.92	2.52	2.34	4.27
	5	2.46	2.74	2.35	3.37	2.78

The results were subjected to routine statistical analysis, taking into account the grouping according to the SPP factor. This included the calculation of typical descriptive statistics, testing for homogeneity of variance across SPP groups, one-way ANOVA by SPP classification, determination of homogeneous outcome groups, and box-plot plotting.

Descriptive statistics

Descriptive statistics (Table 5) included determination of mean values, standard errors (standard deviation of the mean), standard deviations, smallest and largest values, quartiles and medians.

Table 5. Descriptive statistics of adhesion by SPP groups

SPP	ADHESION								
	Cardinality	Mean	SE *)	S *)	Minimum	Q1*)	Median	Q3*)	Maximum
SP1	5	2.31	0.18	0.40	1.69	1.93	2.46	2.63	2.68
SP2	5	2.68	0.09	0.20	2.44	2.47	2.74	2.86	2.92
SP3	5	2.41	0.20	0.44	1.81	2.07	2.35	2.78	3.04
SP4	5	2.35	0.27	0.60	1.87	1.91	2.24	2.86	3.37
SP5	5	3.42	0.27	0.60	2.78	2.96	3.14	4.04	4.27

*) SE – standard error (standard deviation of the mean), S – standard deviation of a single measurement, Q1 – lower quartile, Q3 – upper quartile

Homogeneity of variance

Prior to the analysis of variance, a homogeneity of variance test within the groups was performed to determine whether a variance-smoothing Box-Cox transformation was necessary. Due to the small size of the groups and the lack of reliable information about the normality of the distribution, Leven's test was used. The conducted analysis showed (significance level of the test $p = 0.77$) that there is no need to perform variance stabilization. At the same time, the asymmetry of the positions of the medians in relation to the quartiles observed in the box-plot plot (Fig. 11) justified a posteriori not applying the assumption about the normality of the distribution of results, especially since the group size of 5 is not large.

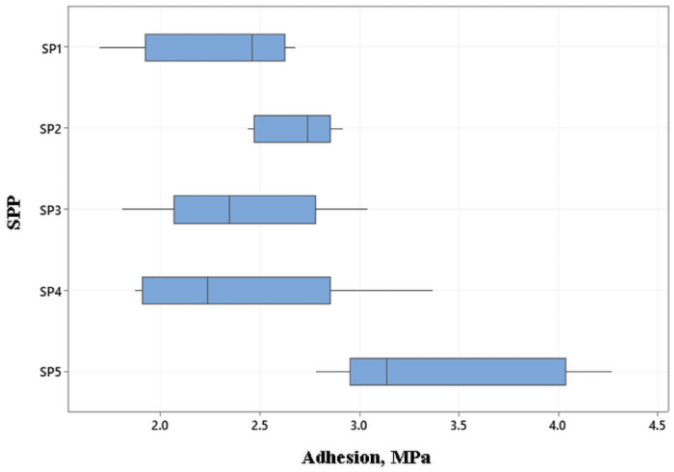

Fig. 11. Box-plot of adhesion against SPP groups

Univariate Anova analysis of variance

The differentiation of the impact of SPP systems was verified using a one-way analysis of variance performed at five levels. It was confirmed that there is a significant differentiation of adhesion depending on the SPP system used (test significance level $p = 0.007$; Table 6).

Table 6. Results of one-factor analysis of adhesion variance with respect to SPP groups

Source	df	SS	MS	F	p
SPP	4	4.29	1.07	4.81	0.007
Error	20	4.46	0.22		
Total	24	8.75			

Homogeneous groups of results

After establishing through the analysis of variance that there is a statistically significant differentiation of adhesion depending on the SPP system used, the question arose between which groups of SPP these differences occur. This means that the so-called homogeneous groups of results.

To determine these groups, Tukey's HSD test of simultaneous testing of differences in mean values was used (Table 7), the results of which were illustrated by a graph (Fig. 12) comparing the position of the confidence intervals of differences with respect to the zero value.

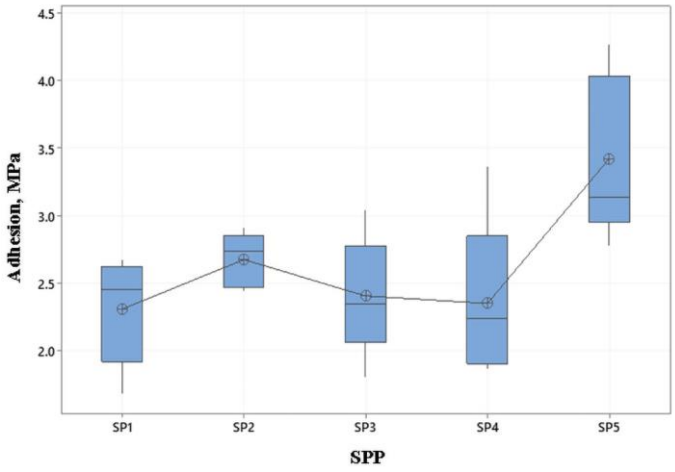

Fig. 12. Box-plot of adhesion against SPP groups with the location of average values in individual groups

Table 7. Table of significance p values of significant differences in SPP groups tested with Tukey's HSD test (significant pairs for $p < 0.05$)

SPP	SP1	SP2	SP3	SP4	SP5
SP1	–	0.74	1.00	1.00	0.01
SP2	0.74	–	0.89	0.81	0.13
SP3	1.00	0.89	–	1.00	0.02
SP4	1.00	0.81	1.00	–	0.01
SP5	0.01	0.13	0.02	0.01	–

The interpretative criterion is checked in one of two ways:

a) whether the value of the significance level p (Table 7) is lower or greater than the assumed significance level α (usually 0.05): if lower, the difference is statistically significant; if greater, the difference is statistically insignificant,

b) whether the zero value (Fig. 13) is contained within the confidence interval of the difference of the average values of a given pair: if it is contained, the difference is statistically insignificant; if not, the difference is significant.

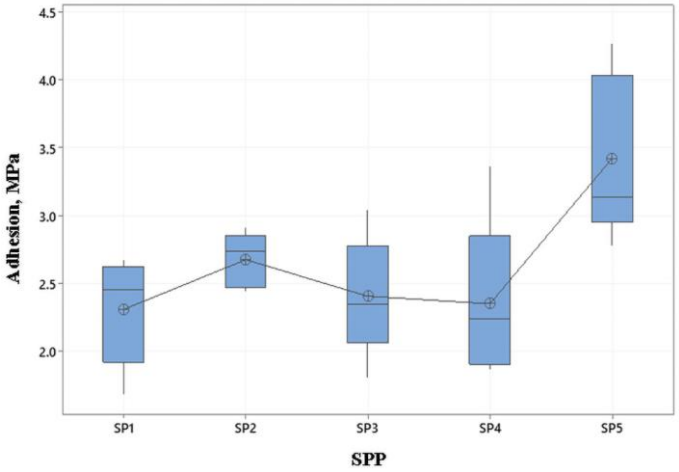

Fig. 13. Differences in mean values in SPP pairs with confidence intervals calculated using the Tukey method

The analysis of the obtained results (Table 7 and Fig. 13) led to the conclusion that there are two homogeneous groups of results (Table 8): one containing SP2 and SP5 and the other consisting of SP1, SP2, SP3, SP4. This pattern of results suggests that it would be advisable to consider additional measurements for SP2 and SP5 to determine whether or not the two painting techniques are statistically different.

Table 8. Determination of homogeneous adhesion groups in SPP grouping

SPP	Cardinality	Average adhesion, MPa	Grouping	
SP5	5	3.42	A	
SP2	5	2.68	A	B
SP3	5	2.41		B
SP4	5	2.35		B
SP1	5	2.31		B

It can therefore be concluded that the SP2 and SP5 coating systems were characterized by the highest adhesion.

3.4. Measurements of specular gloss and colour parameters

A Byk Micro-Tri-Gloss glossmeter (by BYK-Gardner GmbH) was used to assess the specular gloss of the coatings. The tests were performed at the angles of incidence of light radiation (20°, 60°, 85°) in accordance with the standard EN ISO 2813:2014 [23]. There were made 10 measurements for each coating system, which enabled the averaging of test results. Small deviations in the measurement results obtained during the tests resulted from various places where the gloss measurement was made on the test sample. The results of surface gloss measurements of radar-absorbing coatings are shown in Figures 14÷16.

Radar-absorbing coating systems were marked by low gloss of values in the range of 0.2÷9.9 gloss units (GU). The lowest gloss values were found in paint coating systems at the angle of incidence of light α=20° (Fig. 14), and their averaged values were in the range of 0.2÷0.4 GU. On the samples, tarnishing and chalking of the surface layer (SL) of the tested radar-absorbing coating systems were observed. Radar-absorbing coating systems at α=60° obtained average gloss values from 1.4 to 4.0 GU (Fig. 15).

The highest gloss values were found in paint coating systems at the angle of incidence of light α=85° (Fig. 16). According to the assumptions of the Polish Defence Standard NO-80-A200:2021, the gloss of paint coatings made with masking paints should not exceed 8 GU for the observation angle of 85° [29]. The average values of the tested systems ranged from 3.1÷9.9 GU. For the SP1, SP2 and SP4 systems, the gloss values were below 8 GU units, while for the SP3 and SP5 systems they slightly exceeded this value.

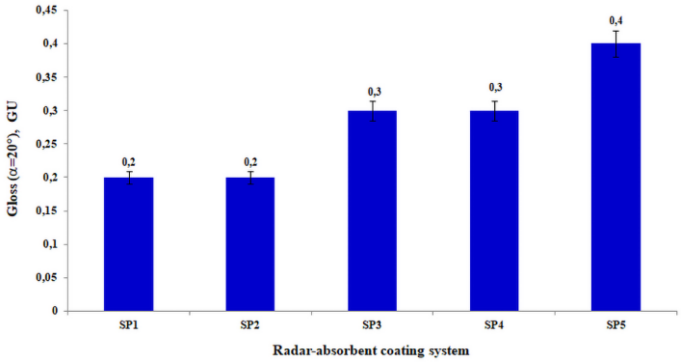

Fig. 14. Gloss of paint surfaces of coating systems at the angle of incidence of light α=20°

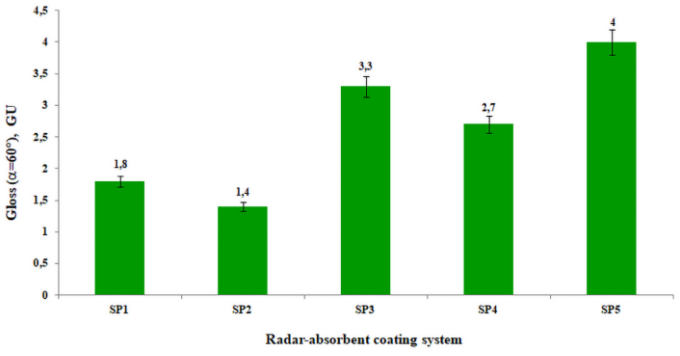

Fig. 15. Gloss of paint surfaces of coating systems at the angle of incidence of light α=60°

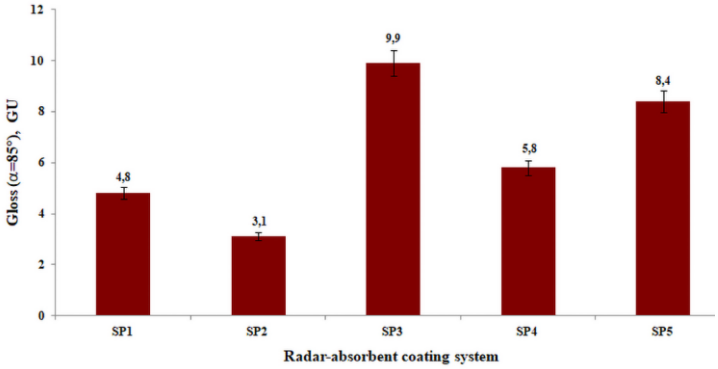

Fig. 16. Gloss of paint surfaces of coating systems at the angle of incidence of light α=85°

Colour is mathematically described with three components: L* – brightness (luminance); a* - component determining the shade from green to magenta; b* - component determining the shade from blue to yellow. The CIELAB colour space is described with the following equations [25]:

$$L^* = 116\sqrt[3]{\frac{Y}{Y_n}} - 16 \quad (2)$$

$$a^* = 500\left(\sqrt[3]{\frac{X}{X_n}} - \sqrt[3]{\frac{Y}{Y_n}}\right) \quad (3)$$

$$b^* = 200\left(\sqrt[3]{\frac{Y}{Y_n}} - \sqrt[3]{\frac{Z}{Z_n}}\right) \quad (4)$$

where:

X_n=94.81 Y_n=100.00 Z_n=107.30 are the colour coordinates of the standard white body.

The method of describing colour using L*a*b* coordinates is currently the most popular and is the basis of colour management systems.

The colour parameters were measured using a CM-700d spectrophotometer (Konica Minolta). During the measurements, the values of individual colour parameters were determined: L*, a*, b* with D65 light and 10° observer [26]. Then, the parameter of colour difference ΔE^*_{ab} relative to the standard was calculated (CIELab values for green color, standard NO-80-A200:2021) according to formula [27]:

$$\Delta E^*_{ab} = \sqrt{(\Delta L^*)^2 + (\Delta a^*)^2 + (\Delta b^*)^2} \quad (5)$$

where:

ΔE^*_{ab} – colour difference between the test sample and the reference sample,

ΔL^* – brightness parameter,

Δa^* – colour parameter,

Δb^* – colour parameter.

From the literature [18, 22] it is known that the colour difference parameter ΔE^*_{ab} with the following values is characterized with:

$0 < \Delta E^*_{ab} < 1$ – the observer does not notice the difference;

$1 < \Delta E^*_{ab} < 2$ – only an experienced observer notices the difference;

$2 < \Delta E^*_{ab} < 3{,}5$ – the difference is also noticed by an inexperienced observer;

$3{,}5 < \Delta E^*_{ab} < 5$ – the observer perceives a distinct colour difference;

$5 < \Delta E^*_{ab}$ – the observer perceives two different colours.

Table 9 shows the colour parameters: L*, a*, b* and the calculated parameters ΔE^*_{ab} for the tested radar waves absorbing coating systems.

Tabela 9. Parametry koloru lakierniczych systemów powłokowych

Sample \ Parameters	L^*	a^*	b^*	ΔE^*_{ab}
Standard green CIELab according NO-80-A200:2021	35.17	-5.14	5.56	-
SP1	35.09	-5.20	5.42	0.17
SP2	37.12	-4.47	7.52	2.85
SP3	33.62	-4.55	4.05	2.24
SP4	34.67	-5.23	4.99	0.76
SP5	34.75	-5.29	5.07	0.67

All tested radar-absorbing coating systems were characterized with ΔE^*_{ab} values below 3.0 (Table 9), which is in accordance with the assumptions of the NO-80-A200:2021 standard. Figure 17 shows the location of the L*, a*, b* components of the tested radar-absorbing coating systems in the CIELab space. The most favourable mapping of colour parameters was obtained for the SP1 paint system -ΔE^*_{ab} = 0.17 (fig. 17a). Despite a slight colour deviation towards blue tones, the parameter ΔE^*_{ab} of the SP4 and SP5 paint systems was below 1 (Fig. 17d and Fig. 17e). The colour difference was within the measurement tolerance, which means that even an experienced observer would not notice the difference between the tested sample and the standard. In the case of two paint systems, i.e., SP2 and SP3, the values of ΔE^*_{ab} were significantly higher than the other systems and amounted to 2.85 and 2.24, respectively. The SP2 paint system was brighter (parameter L* = 37.12) and more yellow (parameter b* = 7.52) compared to the standard parameters, which shows the location of the colour components (Fig. 17b). In the CIELab colour space, the colour of the SP3 radar-absorbing coating system (Fig. 17c) compared to the reference sample was darker (parameter L* = 33.62) and bluer (parameter b* = 4.05).

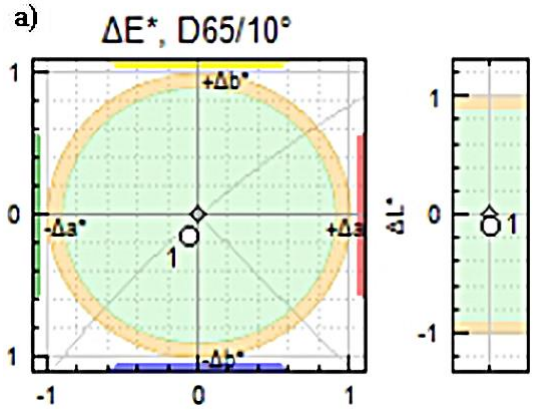

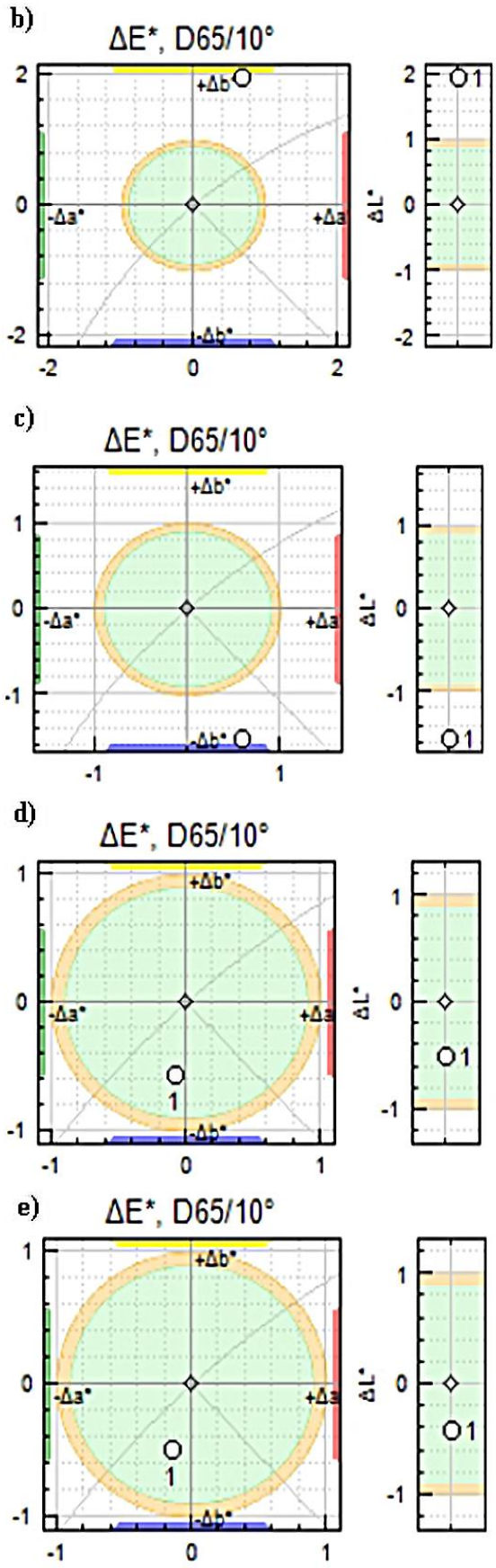

Fig. 17. Location of L*, a*, b* components of paint coating systems in the CIELab space: a) SP1, b) SP2, c) SP3, d) SP4, e) SP5

In the next stage of the research, spectral characteristics of the reflectance were performed using the Jasco V-770 spectrophotometer with 8/d geometry (Jasco). Figure 18 presents the values of the reflectance coefficients of the discussed radar-absorbing coating systems depending on the wavelength of the incident light in the 350-1200 nm range, taking into account the limit values for green special paints for camouflage painting [29].

In the visible light range, the spectral characteristics of the tested radar-absorbing coating systems were within the set parameters, with the exception of the SP2 paint system. SP1, SP4 and SP5 paint systems in the wavelength range of 350-780 nm had a similar course of the reflectance spectrum. In the case of the SP2 and SP3 coating systems, in the above-mentioned wavelength range, a different course can be observed in relation to the other paint systems, which is confirmed by the values of the L*, a*, b* components. At wavelengths of 800÷1200 nm, the lowest reflectance values were obtained for samples SP2 and SP3. Among all the tested radar-absorbing coating systems, the best values of the reflectance coefficient, in relation to the requirements of the NO-80-A200:2021 standard, were shown by the SP1 and SP5 paint systems.

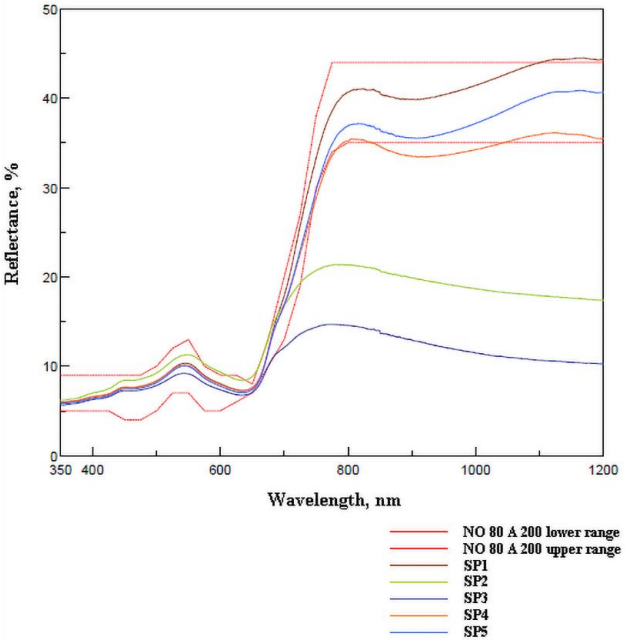

Fig. 18. Values of reflectance coefficients of paint coating systems

4. Conclusions

The analysis and interpretation of the obtained results of operational tests of coating systems allowed the following conclusions to be drawn:

1. The attenuation of radio waves by paint coating systems (containing spherical iron) with increased thickness and variable composition of individual layers exceeds the attenuation of radio waves in the range from 9 GHz to 12.5 GHz currently used in the Polish Armed Forces by multi-band camouflage coatings [28]. The attenuation values obtained for frequencies above 12.5 GHz and in the range from 6 GHz to 9 GHz are within the range required for camouflage coverings known as the Mobile Camouflage Kit (MCK). An undoubted advantage of paint coatings in relation to multi-range camouflage coatings is the integrity of the system with the military facility. It seems reasonable to carry out further work

aimed at optimizing the coating system in terms of operation and determining the zones of a military vehicle that should be protected with a new coating in order to reduce the probability of detection and identification.

2. The SP2 and SP5 radar-absorbing coating systems are characterized by the highest adhesion, while the SP1 system has the lowest adhesion.

3. A very important factor affecting the geometric structure of the coating system is the proper preparation of the base material. Paint systems have a higher roughness in relation to the base material (more than twice). Low values of surface inclination coefficient *Sku* (kurtosis) indicate a large dispersion of surface ordinates. Positive values of the surface asymmetry coefficient *Ssk* (skewness) provide information that we are dealing with a smooth surface without deep scratches (SP2 coating system).

4. The highest gloss values have paint coating systems at the angle of incidence of light α=85°, and their average values are in the range of 3.1÷9.9 GU.

5. Optimal values of the reflectance coefficient in relation to the requirements of the NO-80-A200: 2021 standard are demonstrated by the SP1 and SP5 radar-absorbing coating systems.

6. In the future, the possibility of doping components improving thermal conductivity should be considered. The designed radar-absorbing coating system (taking into account thermal aspects) would make it possible to verify the current view on multispectral camouflage.

References

1. Alenkowicz H, Levitas B. Measurement of complex permittivity and complex permeability of materials. 12th International Conference on Microwaves and Radar. MIKON - 98, Cracow, Poland, 20-22.05.1998: 668-672 (no paper link available).
2. Ašmontas S, Kiprijanovič O, Levitas B, Matuzas J, Naidionova I. Estimation of electrical properties of hidden objects using microwave signals. Materials Science 2014; 2(20): 232-234, https://doi.org/10.5755/j01.ms.20.2.6331.
3. Balakrishnan P, John MJ, Pothen L, Sreekala MS, Thomas S. Natural fibre and polymer matrix composites and their applications in aerospace engineering. Book: Advanced Composite Materials for Aerospace Engineering. Woodhead Publishing Limited, Duxford - Cambridge - Kidlington 2016: 365-383, https://doi.org/10.1016/B978-0-08-100037-3.00012-2.
4. Burakowski T. Areologia – podstawy teoretyczne. Wydawnictwo Naukowe Instytutu Technologii Eksploatacji – PIB, Radom 2013 (no paper link available).
5. Bury M. Obrazowanie obiektów na podstawie wielopunktowej akwizycji mikrofalowych sygnałów szerokopasmowych. Rozprawa Doktorska, Politechnika Warszawska, Warszawa 2009 (no paper link available).
6. Chrzanowski J, Gucma M, Jankowski S, Juszkiewicz W, Montewka J, Przywarty M. Urządzenia radarowe w praktyce nawigacyjnej. Seria Wydawnicza: Urządzenia Nawigacji Technicznej nr 1, Akademia Morska w Szczecinie, Szczecin 2010 (no paper link available).
7. Chung DDL. Materials for electromagnetic interference shielding. Materials Chemistry and Physics 2020; 255: Article 123587, https://doi.org/10.1016/j.matchemphys.2020.123587.
8. Frank F, Tkadletz M, Czettl C, Schalk N. Microstructure and mechanical properties of ZrN, ZrCN and ZrC coatings grown by Chemical Vapor Deposition. Coatings 2021; 11: Article 491, https://doi.org/10.3390/coatings11050491.
9. Jayalakshmi CG, Inamdar A, Anand A, Kandasubramanian B. Polymer matrix composites as broadband radar absorbing structures for stealth aircrafts. Journal of Applied Polymer Science 2019; 136: Article 47241, https://doi.org/10.1002/app.47241.
10. Kotnarowska D. Analysis of polyurethane top-coat destruction influence on erosion kinetics of polyurethane-epoxy coating system. Eksploatacja i Niezawodność - Maintenance and Reliability 2019; 1(21): 103-114, http://dx.doi.org/10.17531/ein.2019.1.12.
11. Kotnarowska D. Powłoki ochronne. Wydawnictwo Politechniki Radomskiej, Radom 2010 (no paper link available).
12. Kowalski S. The influence of selected PVD coatings on fretting wear in a clamped joint based on the example of a rail vehicle wheel set. Eksploatacja i Niezawodność - Maintenance and Reliability 2018; 1(63): 1-8, https://DOI:10.17531/EIN.2018.1.1
13. Kozłowska A. Węzłowe zagadnienia naukowe i techniczne warunkujące rozwój technologii powłok ochronnych w XX wieku. Instytut Mechaniki Precyzyjnej, Warszawa 1987 (no paper link available).
14. Kumar N, Vadera SR. Stealth Materials and Technology for Airborne Systems. Book: Aerospace Materials and Material Technologies. Volume 1: Aerospace Materials. Springer, Singapore 2017: 519-537, https://DOI:10.1007/978-981-10-2134-3.
15. Lazaro A, Girbau D, Villarino R. Analysis of vital signs monitoring using an IR-UWB Radar. Progress in Electromagnetics Research 2010; 100: 265-284, https://DOI: 10.2528/PIER09120302.
16. Levitas B, Matuzas J. UWB radar high resolution ISAR imaging. Second International Workshop Ultrawideband and Ultrashort Impulse Signals (IEEE Cat. No.04EX925) 204: 231-233 (no paper link available).
17. Malshe VC, Sangaj N. Fluorinated acrylic copolymers Part I: Study of clear coatings. Progress in Organic Coatings 2005; 53: 207-211, https://doi:10.1016/j.porgcoat.2005.03.003.
18. Mokrzycki WS, Tatol M. Color, difference Delta E - A survey. Machine Graphics and Vision 2011; 20: 383-411 (no paper link available).
19. Mouritz AP. Introduction to aerospace materials. Book: Introduction to Aerospace Materials. Woodhead Publishing Limited, Oxford - Cambridge - Philadelphia - New Delhi 2012: 1-14 (no paper link available).
20. Ondrejka AR, Kanda M. A time-domain method for measuring the reflection coefficient of microwave absorbers at frequencies below 1 GHz. Antennas and Propagation Society Symposium Digest (IEEE - INSPEC Accession Number: 4239209) 1991: 1656-1659 (no paper link available).
21. Pasieczyński Ł, Radek N, Radziszewska-Wolińska J. Operational properties of anti-graffiti coating systems for rolling stock. Advances in Science and Technology Research Journal 2018; 1(12): 127-134, https://DOI:10.12913/22998624/85705.
22. Plebankiewicz I, Mazurczuk R, Szczodrowska B. Selection and verification of camouflage colours. Materials Research Proceedings 2020; 17: 79-85, https://DOI: 10.21741/9781644901038-12.
23. EN ISO 2813:2014 Paints and varnishes - Determination of gloss value at 20 degrees, 60 degrees and 85 degrees.
24. EN ISO 4624:2016 Paints and varnishes - Pull-off test for adhesion.
25. EN ISO 7724-1:2003 Paints and varnishes – Colorimetry - Part 1: Principles.
26. EN ISO 7724-2:2003 Paints and varnishes – Colorimetry - Part 2: Colour measurement.
27. EN ISO 7724-3:2003 Paints and varnishes – Colorimetry - Part 3: Calculation of colour differences.
28. Norma Obronna NO-10-A208:2014/NO-10-A208:2014/A1:2020 - Pokrycia i komplety maskujące. Wymagania ogólne.
29. Norma Obronna NO-80-A200:2021 - Farby specjalne do malowania maskującego. Wymagania i metody badań.
30. Przybył W, Mazurczuk R, Szczepaniak M, Radek N, Michalski M. Virtual methods of testing automatically generated camouflage patterns created

using cellular automata. Materials Research Proceedings 2022; 24: 69-77, https://DOI: 10.21741/9781644902059-11.
31. Przybył W, Radosz W, Januszko A. Colour management system: Monte Carlo implementation for camouflage pattern generation. Coloration Technology 2020; 136: 407-416, https://doi.org/10.1111/cote.12483.
32. Radek N, Szczotok A, Gądek-Moszczak A, Dwornicka R, Bronček J. Pietraszek J. The impact of laser processing parameters on the properties of electro-spark deposited coatings. Archives of Metallurgy and Materials 2018; 2(63): 809-816, https://DOI: 10.24425/122407.
33. Radek N. Determining the operational properties of steel beaters after electrospark deposition. Eksploatacja i Niezawodność - Maintenance and Reliability 2009; 4(44): 10-16 (no paper link available).
34. Selvakumar N, Barshilia HC, Rajam KS. Effect of substrate roughness on the apparent surface free energy of sputter deposited superhydrophobic polytetra-fluoroethylene coatings: A comparison of experimental data with different theoretical models. Journal of Applied Physics 2010; 108: Article 013505, https://doi.org/10.1063/1.3456165.
35. Toh KB, Todd P. Camouflage that is spot on! Optimization of spot size in prey-background matching. Evolutionary Ecology 2017; 31: 447-461, https://DOI 10.1007/s10682-017-9886-3.
36. Tyrawa P, Kałuski M. Procedury wzorcowania anten pomiarowych. Telekomunikacja i techniki informacyjne 2005; 1-2: 96-115 (no paper link available).
37. Wang D, Zhang B, Jia CC, Gao F, Yu Y, Zhao X, Bai Z. Microstructure and tribological properties of plasma-sprayed WC-17Co coatings with different carbide grain size distribution. Journal of the Japan Society of Powder and Powder Metallurgy 2016; 63(7): 688-696, https://doi.org/10.2497/jjspm.63.688.
38. Wang H, Qiu Q, Gee M, Hou C, Liu X, Song X. Wear resistance enhancement of HVOF-sprayed WC-Co coating by complete densification of starting powder. Materials & Design 2020; 191: Article 108586, https://doi.org/10.1016/j.matdes.2020.108586.
39. Wysocki K, Dąbrowska I, Idziek M. Maskowanie wojsk i obiektów na przykładzie doświadczeń wybranych państw. Akademia Sztuki Wojennej, Warszawa 2020 (no paper link available).
40. Yang X, Xu W, Liu J, Jia Q, Liu H, Ran J, Zhou L, Zhang Y, Hao Y, Liu C. A small-spot deformation camouflage design algorithm based on background texture matching. Defence Technology 2021; 13 October: 1-10, https://doi.org/10.1016/j.dt.2021.10.001.
41. Zhang P, Pang Y, Yu M. Effects of WC particle types on the microstructuresand properties of WC-reinforced Ni60 composite coatings produced by laser cladding. Metals 2019; 9: Article 583, https://doi.org/10.3390/met9050583.
42. https://www.geozondas.lt/list/Seminaras%20Lietuva-Baltarusija.pdf [on-line access 07.09.2022].